Analysis of Water-Soluble Polymers Using Hydrodynamic Chromatography

D. A. HOAGLAND* and R. K. PRUD'HOMME, *Department of Chemical Engineering, Princeton University, Princeton, New Jersey 08544*

Synopsis

Hydrodynamic chromatography (HDC) has been successfully applied to measurements of the molecular size and molecular size distribution of high molecular weight, water-soluble polymers. The scope of the method has been probed by experiments with xanthan, a comparatively stiff polysaccharide, and hydrolyzed polyacrylamide, which possesses a more flexible backbone. Separation occurs during convection of dissolved polymer through the interstitial volume of a chromatography column packed with nonporous beads. Nonequilibrium polymer configurations are readily created by the complex flow between these beads. Such altered configurations strongly affect molecular size measurements. To maximize resolution, hydrodynamic stress must be reduced by employing extremely low flow rates. These low flow rates, particularly important for ultrahigh molecular weight samples, unavoidably lengthen analysis time. Conditions under which chromatograms reflect the size distribution of an injected sample are elucidated. A complete description includes selection of column packing, solvent composition, flow rate, column calibration, and sample detection.

INTRODUCTION

Measurements of the molecular weight and molecular size in solution are frequently difficult for water-soluble polymers with high degrees of polymerization. Quantitative data are therefore sparse, particularly for polyelectrolytes. Although numerous techniques which might close this experimental gap have been explored, a completely satisfactory method has not been discovered. In this contribution we will discuss the potential of hydrodynamic chromatography (HDC) to provide simple and economical size measurements for these often intractable materials. Polymers which are candidates for analysis by HDC are those with molecular weight above several millions. Partially hydrolyzed polyacrylamide, xanthan, DNA, carboxymethyl cellulose, and dextran are examples of polymers which might be studied with the method. These polymers find application in foods, paints, enhanced oil recovery, and water treatment. Although the molecular weight is normally tailored according to the needs of the targeted application, the actual molecular weight of commercial products are often not known accurately. Information about distributions of molecular weight is even more scarce.

Among the molecular weight measurements which have been applied to water-soluble polymers are size exclusion chromatography (SEC),[1] field-flow

*Current address: Department of Polymer Science and Engineering, University of Massachusetts, Amherst, MA 01003.

Journal of Applied Polymer Science, Vol. 36, 935–955 (1988)
 CCC 0021-8995/88/040935-21$04.00

fractionation,[2] sedimentation,[3] birefringence in extensional flow,[4] light scattering,[5] electron microscopy,[6] and viscometry.[7] A fractionation technique such as SEC is often used in conjunction with low angle light scattering to obtain a complete distribution of molecular weight. With other methods, a fractionation step is not employed, and only average molecular weights are readily obtained.

The size and time constraints associated with fractionation of large polymers are severe; these constraints impose fundamental limits on the performance of many common methods for molecular weight measurement. Giddings[8] discusses some of the limitations in the context of SEC of large polymers. Other techniques evade such difficulties more successfully than SEC, but not without the penalty of increased equipment cost and experimental complexity. Holzwarth et al.[9] present a combination of band sedimentation with low-angle laser light scattering; their data for polystyrene sulfonate and polyacrylamidomethylpropane sulfonate represent the state of the art in measurement of molecular weight for water-soluble polymers. The technique, however, appears too tedious for routine use.

Hydrodynamic chromatography, first described over a decade ago,[10] has become an important tool for measurement of particle size in the submicron range. The major advantages of the technique for particle size analysis are rapid experiment time and low equipment cost. The resolution is not especially high, but low resolution can be partially circumvented by deconvolution of data via numerical techniques. Studies with latex particles have shown that HDC is most useful for particles with diameters in the range of 0.05–1.2 μm. Many higher molecular weight, water-soluble polymers will possess sizes in this range.

Theories for particle separation with HDC are reasonably well developed, and a short discussion of these theories is included in a later section. Our primary emphasis will be on the application of HDC to dissolved macromolecules, primarily following an experimental approach. The major differences in HDC separations involving particles and those involving macromolecules are the added complexity in polymer systems of nonspherical shape, deformability, and sample degradation. Adsorption of solute on the packing beads is also a major concern. Finally, with higher molecular weight polymers, detection at ppm concentrations is required to ensure dilute solution behavior. Each of these problem will be considered in a subsequent section, and an optimal strategy for study of polymer solutes will be developed. We have briefly discussed some of these problems in earlier articles;[11,12] Lecourtier and Chauveteau[13] have also described HDC of macromolecules, although in a more limited context.

BACKGROUND

High Molecular Weight Water-Soluble Polymers

The chemical structures of partially hydrolyzed polyacrylamide and xanthan, the polymers to be examined most closely, are presented in Figure 1. Two parameters will normally correlate the dilute solution properties of these types of charged, flexible polymers—the density of charge along the polymer

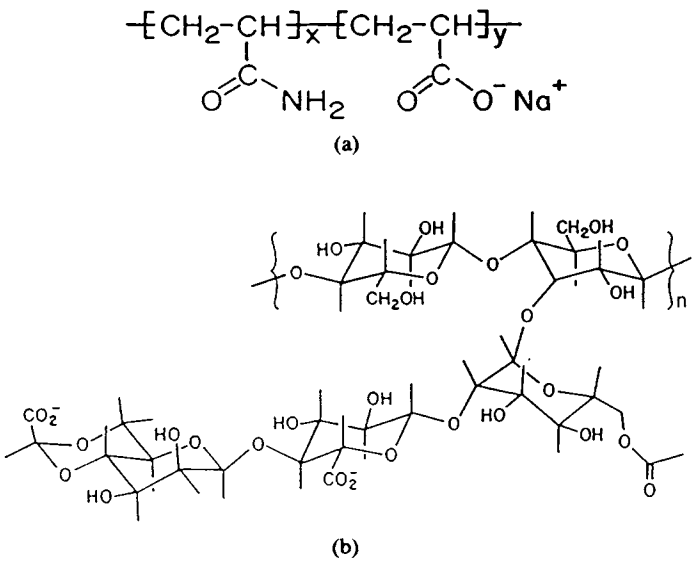

Fig. 1. Chemical structures of partially hydrolyzed polyacrylamide (a) and xanthan (b).

backbone and the molecular weight. An industrial grade polyacrylamide designed as a viscosifying agent might have an average molecular weight which is greater than 5×10^6, with the acrylamide backbone 20–40% hydrolyzed. Polydispersities of 2.0 or greater are usual for this class of polymers; calibration of molecular weight measurements by standards is therefore not feasible as standards are not readily available.

Hydrodynamic Chromatography

Except for the absence of intraparticle porosity in columns employed for HDC, differences between HDC and SEC are minor. HDC columns are packed with monodisperse spherical beads with diameters in the range of 10–30 μm. The nonporous beads form a 3-dimensional void structure which is complex; the initial step in most modeling efforts has been to reduce this structure to a set of equivalent capillaries (Fig. 2). These capillaries will have a radius which is roughly 0.2 times the mean diameter of the packing beads.[14] The ratio of the equivalent capillary radius to the diameter of the solute must be less than about 200 for HDC to be effective. If the flow passage is too small, however, larger solutes are lost because of entrapment.

The model sketched in Figure 2 reveals that the finite size of a solute creates a depletion layer near the capillary wall. In the absence of nonsteric forces, the thickness of the depletion layer depends only on solute size. A solute transported through the tube by flow will sample, under the influence of Brownian motion, all radial positions outside its depletion layer with equal probability. Owing to the monotonic increase of fluid velocity toward the tube centerline, a larger solute travels through the capillary at a greater average velocity than a smaller solute. The ratio of the average solute velocity V_p to the average solvent velocity V_m defines the retention factor R_f:

$$R_f = V_p/V_m \tag{1}$$

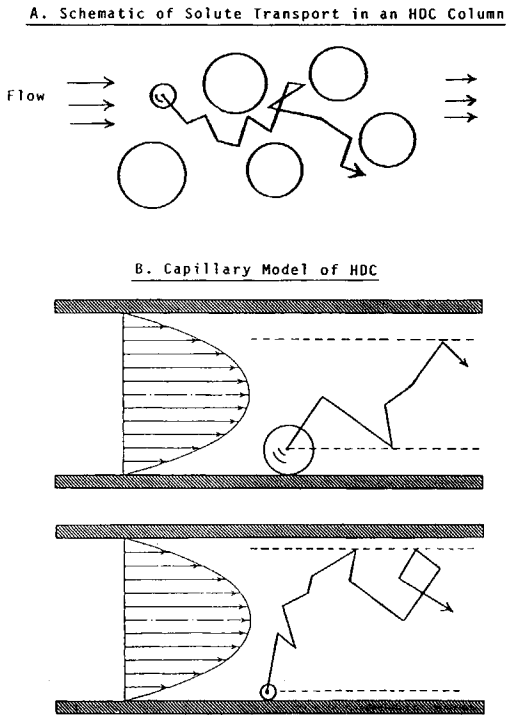

Fig. 2. Schematic of the HDC separation mechanism. The complex structure of a packed bed of spheres, at the top, is reduced to the simple capillary model at the bottom. In the capillaries, transport of two particles with different diameters is followed, illustrating size-dependent depletion layers at the wall. Under Brownian motion the smaller particle can sample a larger fraction of the low velocity region near the wall than the larger particle. (A) schematic of solute transport in an HDC column; (B) capillary model of HDC.

The retention factor is the major characterization of the separation; the primary objective of modeling HDC is to predict the dependence of R_f on experimental variables, most significantly on solute size.

Early experiments with particulate solutes revealed a major impact of wall potentials on the retention factor. In water the potentials are predominately comprised of double-layer repulsions and van der Waal's attractions. Such potentials affect HDC by modifying solute concentration in the critical region near the wall. Concentrations in this region will be governed by a balance of wall potentials and Brownian motion, producing a Boltzmann distribution of solute outside the depletion layer. A theoretical analysis of this phenomenon has been derived for a rigid Brownian sphere translating through a capillary.[15]

The action of wall potentials complicates HDC because separation can depend on the material properties of the packing, solute, and solvent. These properties are generally not known accurately. More importantly, if the relevant properties are a function of solute size, which is expected, the effects of material property variation cannot be isolated from those of size variation. To avoid these difficulties, a "universal calibration" condition is imposed by lowering the solvent's ionic strength.[16] The result is a separation that depends only on the size, and perhaps the shape, of the solute examined.

To understand the universal calibration concept in HDC, it is instructive to examine the electrostatic interaction energy associated with overlapping double layers, which dominate wall potentials when the ionic strength is low. Under these conditions the interaction energy of two unequally sized and widely separated spheres (a packing bead and a rigid translating particle) can be written[17]

$$\Phi(r) = \frac{64\pi\epsilon a_1 a_2 k^2 T^2 \gamma_1 \gamma_2}{(a_1 + a_2)e^2 z^2} \exp(-\kappa r) \tag{2}$$

Here, ϵ is the permittivity of the fluid, a_1 and a_2 are the two radii, z is the counterion valence, and e is the charge on an electron. The double layer thickness κ is given by

$$\kappa = \left(\frac{2e^2 N_A c z^2}{\epsilon kT} \right)^{1/2} \tag{3}$$

where N_A is Avogadro's constant and c is the concentration of electrolyte. Finally, γ_1 and γ_2 are functions of the two surface potentials ψ_1 and ψ_2, respectively:

$$\gamma_i = \frac{\exp(ze\psi_i/2kT) - 1}{\exp(ze\psi_i/2kT) + 1} \tag{4}$$

If the two dimensionless surface potentials $ze\psi_i/kT$ are large, γ_i goes to 1.0. The interaction energy of the two spheres is no longer a function of surface potential—universal calibration in HDC can exist since the electrostatic interactions depend only on solute size.

The conditions for universal calibration are low ionic strength and high surface potential. These conditions are the reverse of those normally imposed to obtain universal calibration in aqueous SEC. With sulfonated ion-exchange resins, which are the most common HDC packing materials, universal calibration is obtained with latex particles at ionic strengths below about 2×10^{-3} M.[18] (The column in this study has also been packed with an ion exchange resin.) The evaluation of the universal calibration method for charged polymers, to be discussed later, is more complicated.

Despite its simplicity, the current model for particle HDC is reassuringly successful. The good agreement with experimental data for spherical particles firmly demonstrates that the fundamental nature of HDC is understood.[18] The remainder of the paper describes efforts to put HDC separations of high molecular weight polymers on a theoretical and experimental basis comparable to that available for separations involving particles.

EXPERIMENT

Equipment

An apparatus employed for HDC (Fig. 3) contains nearly the same components as a conventional SEC. The quality of HDC separations depends chiefly

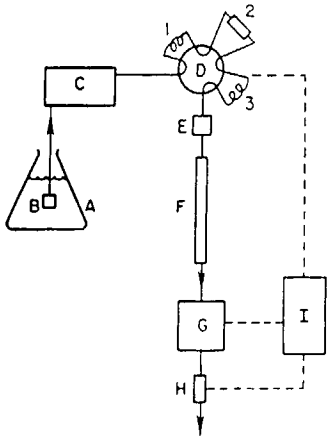

Fig. 3. HDC apparatus: (A) solvent reservoir; (B) 2-μm prefilter; (C) pump and pulse dampener; (D) injection valve [(1) marker or delay sample loop; (2) spacer column; (3) polymer sample loop]; (E) 2-μm column prefilter; (F) HDC column; (G) fluorometer or UV/visible detector; (H) siphon flow meter; (I) computer and data collection hardware.

on the performance of the pump, injection valve, and column packing. Maintenance of steady flow by the pump is extremely important as the variation of elution volume between solutes of different size is small. The pump selected for this demanding application, in conjunction with a microflow control module, has provided a 4 orders-of-magnitude range of flow rate, 1.0 μL/min–10.0 mL/min (Model M45, Waters Associates, Milford, MA). The flow rate is routinely monitored with a homemade siphon flowmeter. This device measures flow by gathering a known quantity of fluid in a small reservoir. When the reservoir is full, the gathered fluid is released automatically, and the elapsed time from the previous release is recorded. These time intervals, in combination with the known reservoir volume, provide several flow rate measurements over the duration of an experiment. The flow rate during a run is observed to vary by no more than 0.3%, the same variation observed in average flow rate between separate runs at the same pump setting.

Samples are introduced into the flow stream via a 12-port injection valve (Valco Instruments, Houston, TX) fitted with two sample loops and a spacer column. When an experiment is initiated, fluid from both loops is injected into the flow stream at the same time. One loop contains material which elutes directly onto the main HDC column; fluid from the other loop first flows into the spacer column, producing a time delay before introduction onto the HDC column. The 2.0 mL spacer column is packed with 30 μm Zipax glass beads from DuPont Instruments (Wilmington, DE). The loop providing direct injection into the main column is normally used to introduce a polymer sample into the flow stream. The second, delay loop places a low molecular weight marker into the flow at a point upstream of the polymer sample. The delayed marker injection technique[19] provides an internal standard for each run because the low molecular weight marker injected from the delay loop should elute at the same relative position in each experiment. This "reference" is an easy way to establish the reproducibility of the system and to increase the accuracy of measured elution times. The markers employed for runs

reported in this article are 8-hydroxy-1,3,6-pyrene trisulfonic acid (Kodak, Rochester, NY) and potassium dichromate.

A single stainless-steel chromatography column, 1.00 cm diameter by 24.8 cm long, has been packed with a specially fractionated Dowex50W (X16) cation exchange resin (a gift of H. Small, Dow Chemical, Midland, MI). This material is highly crosslinked as a result of polymerization of the styrene-based resin in the presence of 16% divinylbenzene. The ion exchange resin is highly sulfonated, establishing an elevated negative charge density throughout the resin at neutral pHs. The measured average particle diameter is 11 μm.

The porosity of this column is 0.272 ± 0.005, which is low for a packed bed of solid spheres; the limiting porosity of a bed of spheres in a close-packed structure is 0.26. It is unlikely that the column's porosity could so closely approach the close-packed limit without significant extraneous packing effects. Two phenomenon could conceivably be responsible, the polydispersity of the packing or deformation of packing beads to nonspherical shape. The low porosity has apparently not impaired the usefulness of this column, which was graciously packed for us by Marty Langhorst (Dow Chemical, Midland, MI).

During preliminary phases of this project several different column types were tested for HDC suitability. These included a sample of glass spheres (Potters Industries, Hasbrouck Heights, NJ) fractionated to 30 μm average diameter; the glass spheres proved unsatisfactory because of a steady pressure increase with time. The same problem, although much less severe, arose when a column packed with 27 μm Zipax spherical silica beads was tested. As with the glass spheres, the pressure increase made experiments irreproducible. A polystyrene/divinylbenzene resin obtained from Dyno Particles A.S (Lillestrom, Norway) was also studied, again with little success. This 14.8 μm diameter resin apparently contained some intraparticle porosity which was observed to fluctuate between successive runs. The Dowex50 ion exchange resin finally selected for subsequent work exhibited none of the problems encountered with the other materials, and the original column is still functioning properly after 2–3 years of steady use.

Both fluorescence and ultraviolet/visible absorption have been employed to detect eluting solute. With high molecular weight polymers, low concentrations are most easily detected with fluorescence; with particles, turbidity, measured by attenuation of UV light, is the more sensitive measure of concentration. A fluorometer (Model FS 970, Kratos Analytical, Ramsey, NJ) and a UV/visible detector (Model 788, Micromeritics Instruments, Norcross, GA) possessing similar internal volumes have been used interchangeably as needed. Output signals from both the fluorometer and the UV/Visible detector are connected to a Hewlett-Packard 85 microcomputer through an A/D interface (Model 760, Nelson Analytical, Cupertino, CA). Over a typical chromatographic run 800 data points are stored, approximately 200 of these spanning the sample peak in the chromatogram. The computer is also interfaced to the injection valve and siphon flowmeter.

Mobile Phase

The proper selection of mobile phase is a critical step in any chromatographic analysis. The selection is especially important in aqueous separations

of high molecular weight polymers because potentially large interactions with the packing material are controlled by solvent composition. Some of the constraints in HDC are rather severe. A satisfactory mobile phase should:

1. Possess low ionic strength.
2. Minimize polymer adsorption.
3. Provide good solvent quality.
4. Contain no components which specifically interact with functional groups in the polymer.
5. Produce a stable detector signal.

The ability to use a single composition for several different polymers species would be advantageous.

The first two constraints, low ionic strength and minimal adsorption of solute, are the most restrictive. In aqueous solutions, adsorption of both polymers and particles can be sharply reduced by addition of low concentrations of surfactant. Solute adsorption from these solutions is significantly hindered by dense barriers of adsorbed surfactant. Complete surfactant surface coverage, and thus drastically reduced adsorption of solute, generally occurs only at surfactant concentrations above the critical micelle concentration (CMC). The requirement in HDC of low ionic strength dictates the use of a nonionic surfactant for adsorption protection. Triton X-100 (Rohm and Haas, Philadelphia, PA) has been found effective at 2 g/L, about four times its CMC.[20] Substantial evidence indicates that the linear hydrophilic portion of the surfactant is fully extended outward from the surface at concentrations above the CMC, and that for this type of surfactant the steric barrier is from 2 to 4 nm thick.[21]

The mobile phase also contains $0.002M$ NaN_3, added as a bactericide. The total ionic strength is therefore only $0.002M$, sufficiently low to ensure the validity of universal calibration for particle HDC. An alternative to obtaining universal calibration with polymers, even at high ionic strengths, is to adjust the pH to the pKa of the polymer. With no molecular charge at this pH, the size measured by HDC is not a function of the material properties of the polymer; strong electrostatic forces are absent. There are two mild objections to this approach. First, a new mobile phase must be developed for each polymer species. Second, for many water-soluble polymers the neutralization of charge puts the polymer near its theta state, and precipitation is then a danger. A successful HDC study of hydrolyzed polyacrylamides has employed this technique.[22]

The low ionic strength solutions prepared with 2 g/L Triton X-100 and $0.002M$ NaN_3 are stable; solution properties of refrigerated samples have remained constant for months. One final consideration is the possibility of specific interactions between low molecular components and the polymer. Such interactions have not been characterized for the polymer systems studied here; some evidence indicates that polymers containing weak acid groups may form hydrogen bonds with polyoxyethylene surfactants and that this binding may either reduce or expand molecular size depending on surfactant concentration and pH.[23] Such effects, however, are not likely to be large and can be ignored here.

Labeling and Detection of Polymer Solutes

Many water-soluble polymers can be detected at extremely low concentration by fluorescence from attached labels. In this study a fluorescein derivative is attached to a small percentage of the carboxyl groups in xanthan and hydrolyzed polyacrylamide.[3] An acceptable signal-to-noise ratio is thereby obtained with the fluorometer for either polymer at injected concentrations as low as 5 ppm. Such low concentrations can be measured with the fluorometer set to 460 nm excitation and detection at all wavelengths over 500 nm. This tagging procedure modifies only a small fraction of the carboxyl groups in the polymer; IR spectroscopy and conductometric titration have demonstrated that the carboxyl content of partially hydrolyzed polyacrylamides is vitually unchanged by tagging. HDC data have been obtained primarily with two samples: an unmodified xanthan (Kelco, San Diego, CA) and a commercial polyacrylamide, designated SF210, with a carboxyl substitution of 9.5% and a nominal molecular weight of 12–15 million (Superfloc 210, American Cyanamid, Stamford, CT). The xanthan sample probably has a weight-average molecular weight in the range $2–4 \times 10^6$.

RESULTS

Polymer Adsorption on the Column Packing

The mobile phase discussed in the Experimental section has been designed primarily to minimize polymer adsorption. Polymer loss has been tested for each injection by comparing the injected polymer mass to the eluted polymer mass. The recovery of xanthan at 1.0 mL/min is $95 \pm 5\%$. Similar recoveries of tagged polyacrylamide are observed, and the recovery appears independent of flow rate for both polymers. A dependence of recovery on concentration is also not observed. If measured recoveries were lower, peaks shapes would be distorted as a result of preferential and irreversible[24] adsorption of higher molecular weight fractions.

Polymer Concentration

Injection of samples which are not truly dilute could produce three negative effects in HDC. First, meaningful interpretation of data is only possible when polymer concentrations are low enough to ensure negligible "crowding" of neighboring molecules. Second, only at dilute concentrations are polymeric contributions to hydrodynamic stress sufficiently unimportant to maintain a concentration independent velocity field in the interstitial pore volume. Finally, a linear relationship between injected concentration and detector response is desirable. Unlike other types of chromatography, the second concentration effect is likely to be the most restrictive since the velocity field plays an integral role in the separation. For these reasons the influence of concentration on polymer separations has been closely examined.

Figure 4 demonstrates the linearity of detector response with injected concentration for both tagged xanthan and tagged, hydrolyzed polyacrylamide. At these concentrations and signal levels such linearity is expected. Figures 5 and 6 demonstrate that both the location and height of peaks shift

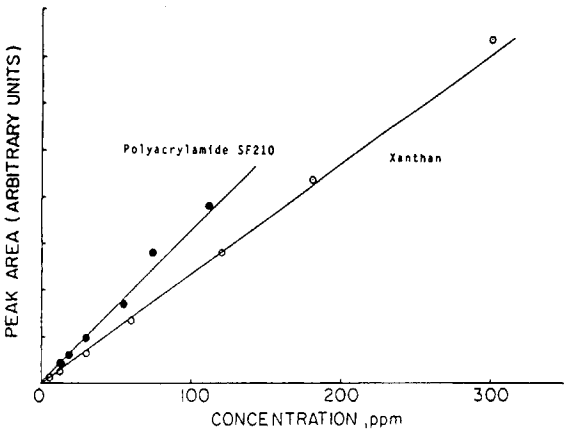

Fig. 4. Demonstration of linear fluorometer response with respect to injected polymer concentration.

as polymer concentration is increased. The changes in peak location can be most closely associated with increasing molecular overlap at higher concentration levels. Changes in peak height are not as easily interpreted, but the effect of the polymer on the flow field is likely the most important cause. If the polymer concentration is too high, "viscous fingering" can broaden peaks and create nonlinearity between concentration and peak height. Viscous fingering is a result of the hydrodynamic instability arising from displacement of a less viscous solvent by a more viscous solution, which in this case is the injected sample.

Molecular overlap and viscous fingering are difficult to predict in these situations because theories for nondilute solution behavior are restricted to quiescent conditions.[25,26] In HDC the solution is flowing and, although ap-

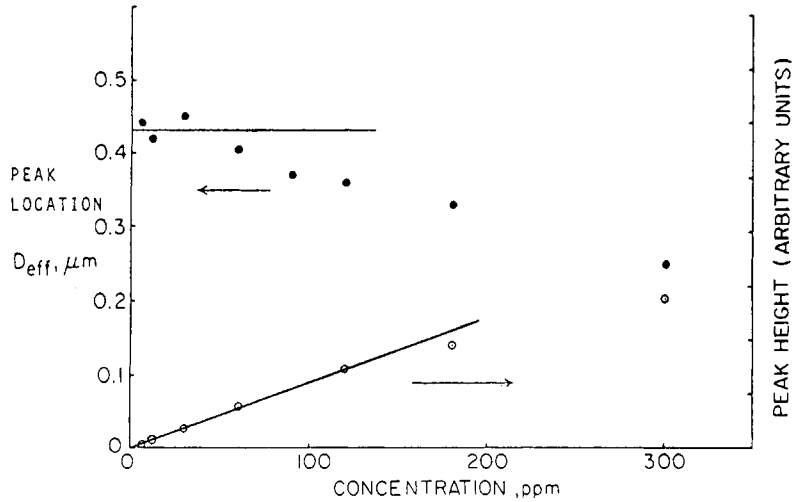

Fig. 5. The position and height of the peak maximum for xanthan as a function of injected polymer concentration. The peak maximum position is expressed in terms of the effective polymer size D_{eff}. The flow rate is 0.5 mL/min.

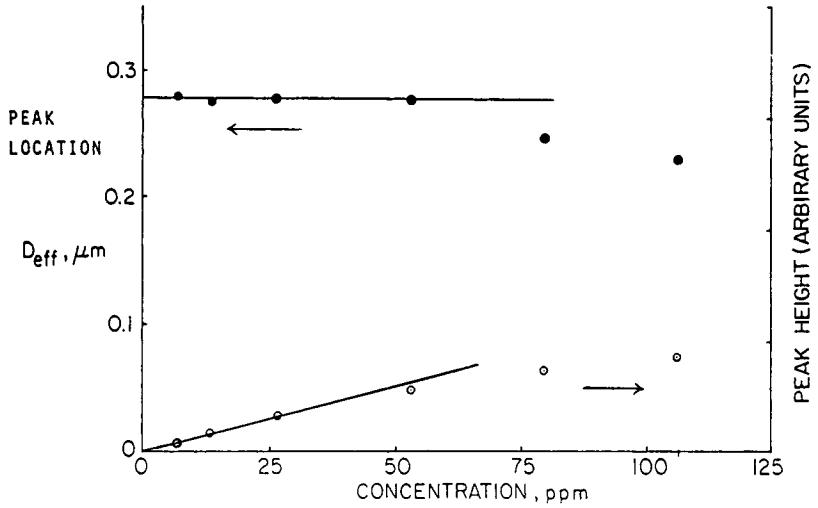

Fig. 6. The position and height of the peak maximum for polyacrylamide SF210 as a function of injected polymer concentration. The peak maximum position is defined by the effective polymer size as in Figure 5. Once again, the flow rate is 0.5 mL/min.

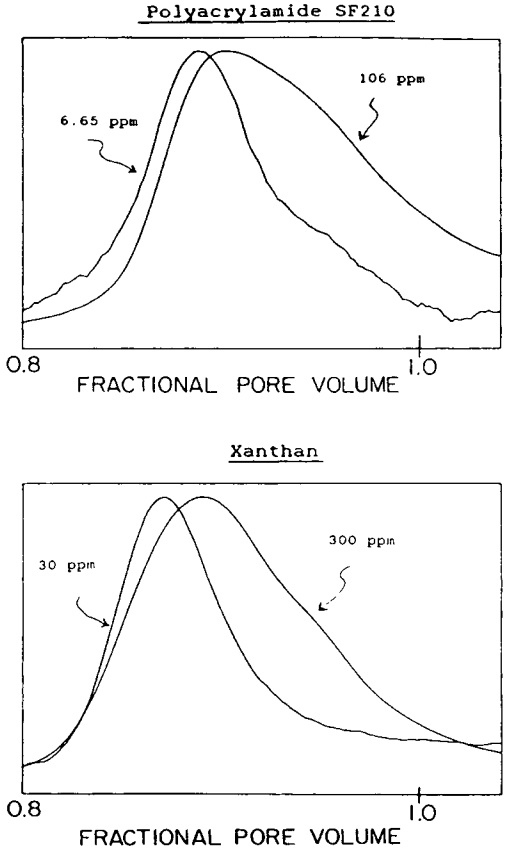

Fig. 7. Examples of the concentration dependence of peak location and peak shape for polyacrylamide SF210 and xanthan. The flow rate for all four runs is 0.50 mL/min.

pearing dilute in many properties, may exhibit strong non-Newtonian rheology.[27] For the polyacrylamide both peak height and location become concentration-dependent for injected concentrations above 50 ppm. For xanthan these parameters become concentration dependent above 100 ppm. The concentrations at which nondilute behavior in HDC are first observed appear to be about twice the critical overlap concentration C^* determined, for example, by the intrinsic viscosity.[28] A standard injected concentration of 60 ppm for xanthan and 50 ppm for the polyacrylamide have been established with the help of data in Figures 5 and 6.

Figure 7 more directly shows how the position and shape of peaks change with concentration for both polymers. A small shift in peak location for nondilute samples is clearly seen, while more dramatic effects are noted in the peak shape. The nonlinearity of the peak height with injected concentration is observed to arise from the development of a tail on the peaks at higher concentrations. Peak tailing is consistent with viscous fingering as the dominant concentration effect.

Calibration

Molecular sizes will be reported relative to particle standards owing to the lack of suitable polymer standards in the molecular weight range of interest. The validity of universal calibration for particle analysis using this HDC system has been verified experimentally, with the results plotted in Figure 8. The dimensionless surface potential of the packing beads is 3–5,[29] and the particle calibration standards have surface potentials in a similar range. Such potentials, when considered with the known ionic strength of the solvent, are consistent with predictions of universal calibration from the equivalent capillary model.

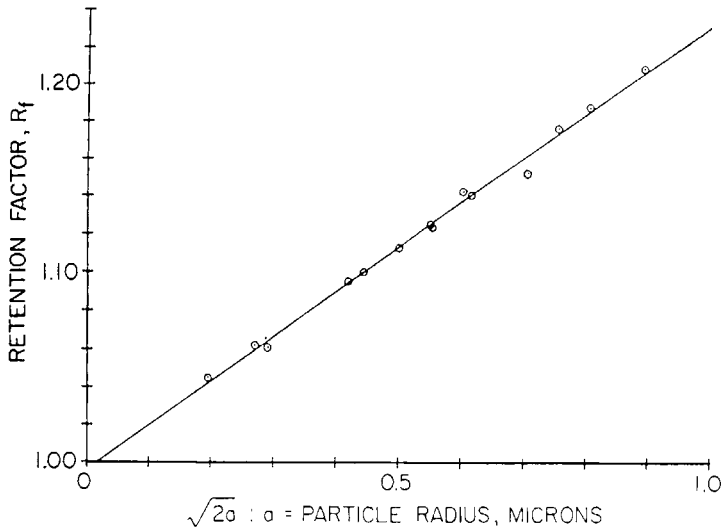

Fig. 8. Column calibration measured with latex particle size standards. Packing: Dowex50 (X16); mobile phase: 2 g/L Triton X-100, 0.002M NaN_3.

It is difficult to prove that universal calibration exists for the polymer separations as well. An approximate surface potential for the polymer can be calculated by assigning to the polymer coil a hard sphere diameter of twice the polymer's radius of gyration and assuming all charge resides on the sphere surface. For the electrolyte concentration employed, $0.002M$, the dimensionless surface potential calculated in this fashion is near unity. The value is approximate since both the charge density of the polymer and its appropriate diameter can be estimated only crudely. Without the availability of a more sophisticated theory of polymer–particle interactions, we will make a physically reasonable approximation that universal calibration has been obtained for polymer separations when such conditions have been established for particle separations. Only by coupling the HDC apparatus to a technique of absolute size measurement, such as low angle light scattering, could this assumption be rigorously tested. Light scattering has recently been employed in HDC.[22]

The particle standards used in preparation of Figure 8 exhibit a wide disparity of surface charge density and were purchased from a variety of sources (Polysciences, Warrington, PA; Duke Scientific, Palo Alto, CA; Interfacial Dynamics Corp., Portland, OR). The single empirical line correlating all data is a verification of the universal calibration concept in HDC. The polymer size D_{eff} is determined by combining this calibration curve with the polymer's retention factor. Similar particle/polymer calibrations have been employed in SEC.[30] Figure 8 spans most of the size range important to polymer study. Latex particles larger than 0.9 μm do not elute from the column so that some extrapolation is necessary to obtain size measurements on larger polymers. It is difficult to see how the error arising from this extrapolation can be quantitatively estimated, and it is assumed here to be small.

Flow Effects

For deformable or nonspherical solutes it is not unreasonable to expect HDC separations to depend strongly on flow rate as a result of stress-induced changes in polymer configuration. The deformation of flexible polymers and orientation of nonspherical polymers are likely to be greatest at high flow rates (which, in a porous column, are equivalent to high elongational strain rates). If either deformation or orientation occur during analysis by HDC, the measured size is more difficult to interpret than the sizes determined for rigid particles. We expect, however, that if the strain rate (i.e., the flow rate) is low enough, the polymer's rotary Brownian motion will cause the configuration to be outlined by a spherical envelope. The diameter of this envelope D_{eff} will be the parameter measured by HDC. For larger strain rates D_{eff} will reflect a flow contribution arising from the nonsphericity of the polymer.

A more complete description of the dynamics of polymer solutes in the interstitial volume of an HDC column is to be published elsewhere. Only the more practical implications of flow-dependent HDC behavior will be discussed here. Flow-dependent data is obviously difficult to interpret and should be avoided whenever possible. Flow effects are reduced by decreasing the flow rate; lowering the flow rate, however, will increase the time necessary to

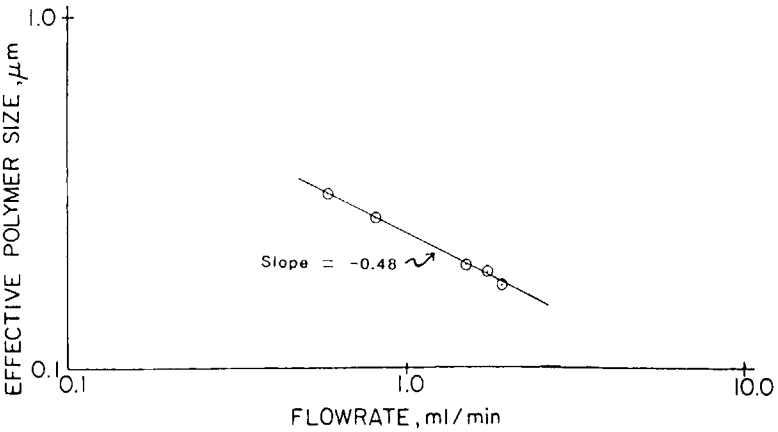

Fig. 9. The effect of flow rate on the elution of tobacco mosaic virus particles.

analyze samples and perhaps eliminate the time advantage HDC has over other techniques.

To clearly illustrate the effects of deformability and orientation in HDC, three solute types have been studied in detail: tobacco mosaic virus (TMV), a rigid rodlike particle of submicron dimensions (a gift of Prof. Charles Stevens, Univ. of Pittsburg); partially hydrolyzed polyacrylamide; and xanthan, carefully prepared to prevent denaturation.[31] Xanthan molecules adopt a conformation between that of TMV and polyacrylamide, existing in solution as stiff "wormlike chains" with contour lengths on the order of 10–20 times the persistence length of the molecule.[5] Hydrodynamic effects are observed by varying the column flow rate and observing changes in the effective size of the polymer. As the solute is oriented or deformed by flow, the dimension measured by HDC, which is a dimension transverse to the direction of flow, is expected to change.

Figure 9 displays the decrease of effective diameter of TMV particles as the flow rate in the column is increased.[32] Even at the lowest flow rate shown, the virus is not fully relaxed but maintains some orientation in the direction of flow. At still lower flow rates the rodlike particle will tumble randomly as a result of rotary Brownian motion; such motion causes the molecule to describe a spherical envelope with a diameter of approximately the particle length. The size of this envelope, and thus the size measured by HDC, will be independent of flow rate in the low flow rate regime. Lecourtier and Chauvateau[13] have presented a more rigous theory for the low flow rate behavior of rodlike particles in HDC.

Orientation effects are observed for TMV under conditions which are typical in chromatography of large polymers or particles; the experiments have not been manipulated to emphasize the importance of flow. Clearly the behavior shown in Figure 9 is undesirable for size analysis since the particle size depends so strongly on flow rate. Without knowing *a priori* the geometry of the particle and how this geometry behaved in an HDC experiment, the measurements shown in Figure 9 would reveal little about the size of the TMV particles. Electron micrographs of the TMV sample reveal a mean particle length of 0.7 μm.[32]

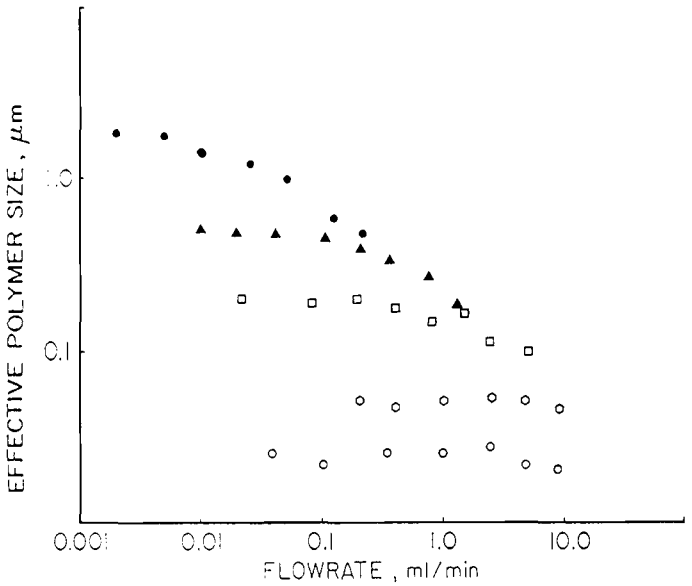

Fig. 10. The effect of flow rate on the elution of polyacrylamide SF210. Degradation of polymer during the analysis occurs in each case at flow rates just above those shown. Unmodified molecular weight = 12–15 × 10^6; carboxyl substitution = 9.5%. (●) Unmodified; (▲) sheared 30.0 min; (□) sheared 12 h; (○) sonicated 1.0 min; (○) sonicated 5.0 min.

An extensive collection of flow data for the polyacrylamide SF210 is shown in Figure 10. Each of the curves correspond to a different molecular weight. The samples have been prepared by degrading the original material by sonication or high shear stirring. Sonication is used to obtain highly degraded samples, while shear mixing at high speeds produces a less severe effect. All of the curves show a low flow rate plateau of D_{eff}, indicating an equilibrium configuration. Above the critical flow rate at which deformation begins, the molecular size measured by HDC decreases. The vertical spacing between curves changes in this flow rate range. This change in spacing implies that the separation efficiency of HDC for flexible molecules is highest at low flow rates. The importance of this behavior in calculating molecular size distributions is discussed in a later section.

Finally, Figure 11 shows the dependence of D_{eff} on flow rate for the somewhat rigid and rodlike polymer xanthan. This data is quite similar to that taken with polyacrylamide SF210; a low flow plateau in size gradually yields to a flow-dependent size as the flow rate increases. For xanthan the molecular basis of the flow-dependent behavior probably includes both orientation and deformation by the flow field.

The xanthan data, as well as that taken for partially hydrolyzed polyacrylamide, show the appropriateness of HDC for size measurements of industrially important water-soluble polymers. The range of the technique closely approximates the distribution of molecular size for these polymers. Flow effects can obviously have a pronounced and negative impact on the quality of data.

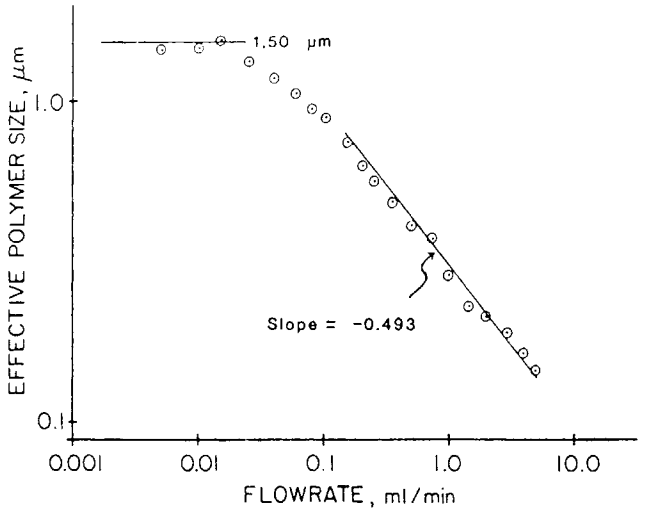

Fig. 11. The effect of flow rate on the elution of xanthan. As discussed in the text, degradation has been observed at flow rates above 5 mL/min.

Degradation

Mechanical degradation attributable to flow stresses is often a serious problem when polymer solutions are made to flow in porous materials. Since these stresses also cause molecular deformation, it might be expected that degradation would occur under conditions similar, although perhaps more severe, to those causing deformation. Despite its significance, degradation is often neglected when analyzing chromatographic separations of high molecular weight polymers.[33,34] When degradation does occur, interpretation of chromatographic data is impossible. To ensure the validity of molecular size and molecular size distributions obtained from the experiments described here, a study of degradation has been undertaken using sample reinjection experiments.

In the reinjection experiments a large volume of polymer solution (2.0 mL) is first injected into the column at the test flow rate; the central part of the eluated slug is then collected. A portion of the collected material is reinjected at a flow rate lying in the low flow size plateau of the original sample. If the reinjected material has a size corresponding to values on the plateau, degradation most likely has not occurred at the test flow rate. If, however, the reinjected sample has a D_{eff} below its original value, the polymer has certainly been degraded by flow.

All of the data plotted in Figures 10 and 11 have passed the reinjection test and are believed to accurately reflect the behavior of the injected polymer. Much of the original data did not pass the test and is therefore not plotted in these figures; each curve terminates, at the high flow rate end, where degradation has been observed. The transition from experiments in which degradation is not observed to those where degradation does occur is not reflected in any obvious way in the original chromatographic data; degradation is only apparent in the context of the reinjection experiments.

Molecular Size Distributions

The size distribution of xanthan in its equilibrium state as determined by HDC is shown in Figure 12. To obtain this data the column flow rate has been reduced to 5.2 μL/min, with a corresponding run time of 13 h for the xanthan peak and 25 h for the entire experiment. These are close to the maximum run times possible with the apparatus because of baseline drift and noise. The chromatogram, also shown in Figure 12, has been directly translated into a size distribution using the particle calibration curve; no dispersion correction has been attempted. The xanthan sample has both number- and weight-average sizes between 1.0 and 2.0 μm, but there is some material in the 4–5 μm range. The size polydispersity for this peak is 1.5, although there is a large uncertainty since this value is extremely sensitive to the baseline selected.

The polydispersity in size for xanthan is reasonable in light of previous results on the molecular weight distribution of this polymer, which indicate a molecular weight polydispersity of 1.4–1.7.[35,36] The relationship between the size polydispersity and the molecular weight polydispersity depends on both the conformation of the polymer in solution (which determines the depen-

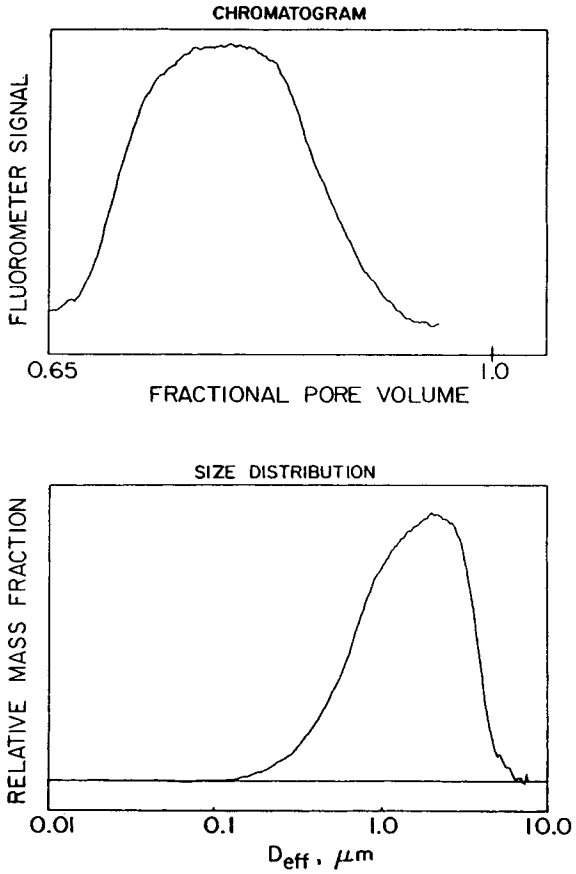

Fig. 12. The chromatogram of xanthan in the low flow rate plateau, and the corresponding size distribution. The weight- and number-average sizes are 1.94 and 1.28 μm, respectively.

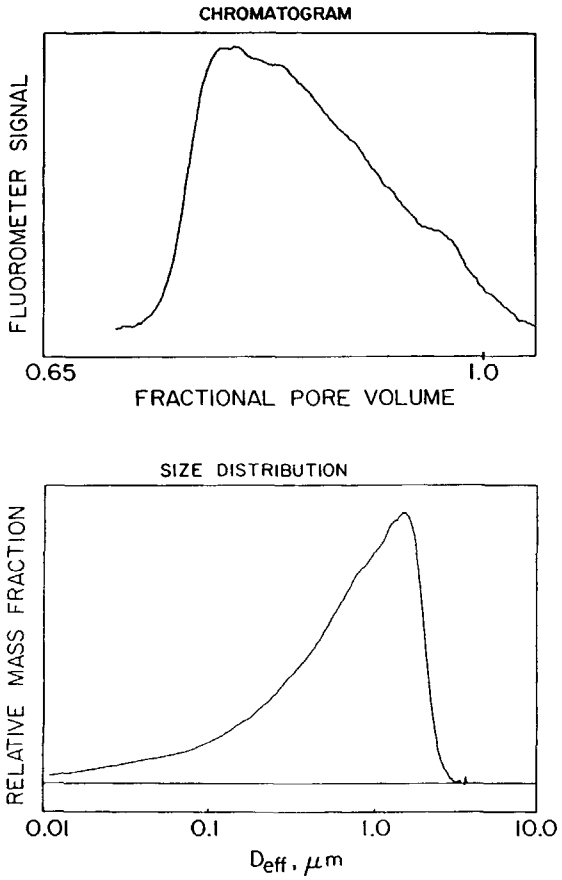

Fig. 13. The chromatogram of polyacrylamide SF210 in the low flow rate plateau, and the corresponding size distribution. The weight- and number-average sizes are 1.02 and 0.37 μm, respectively.

dence of molecular size on molecular weight) and the details of the molecular weight distribution. The polydispersity in molecular weight is always larger than the polydispersity in molecular size so that the results presented here are consistent with the cited literature values.

The size distribution of the polyacrylamide SF210 sample at equilibrium has been plotted alongside the corresponding chromatogram in Figure 13. Again, an extremely low flow rate is necessary with this polymer to ensure a fully relaxed conformation during elution from the column. The number- and weight-average sizes are between 1.0 and 2.0 μm, and the size polydispersity is about 1.7. One of the major drawbacks to HDC is relatively large column dispersion, which reduces resolution. The main impact of dispersion in Figure 13 is to increase the apparent fraction of low molecular weight polymer. The broadening of the peak on the low molecular weight side of the chromatogram overemphasizes this material in the final size distribution. The skew in the effect of dispersion on the size distribution arises from the nonlinearity of the calibration curve (see Fig. 8).

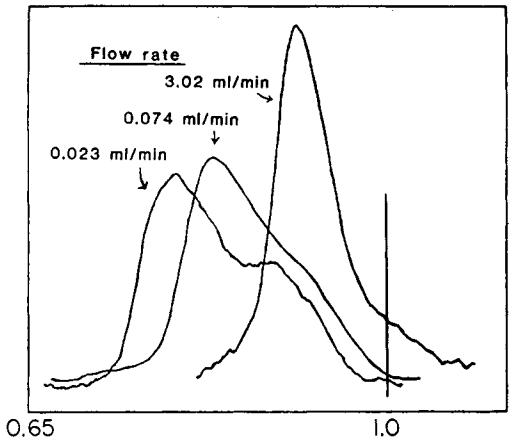

Fig. 14. The chromatograms of a degraded, bimodal sample of polyacrylamide SF210 as flow rate is varied. The clearly bimodal size distribution, observed at 0.023 mL/min, is not obvious at higher flow rates.

The molecular sizes determined by HDC seem to be larger than those provided by other methods such as quasielastic or low angle light scattering. Unfortunately, no data from these methods are available for our samples. Although a number of assumptions have been necessary to obtain the HDC sizes, we believe that the HDC results are reflective of the molecular dimensions at low ionic strength. Scattering techniques have been applied to similar samples at higher ionic strengths,[5,37,38] conditions leading to reduced chain dimensions.

A clear example of the ability of HDC to determine a molecular size distribution is demonstrated in Figure 14, which presents chromatograms for a degraded polyacrylamide SF210 sample as the flow rate is varied. The degradation has been induced by sonicating the dilute polymer solution for a time corresponding to intermediate levels of degradation. Many previous studies have shown that sonication leads to bimodal molecular weight distributions at these levels of degradation.[39] The importance of low flow rate in increasing resolution is easily seen in the data. At the highest flow rate the chromatogram gives little indication of the bimodal nature of the sample. The low flow rate chromatogram, however, clearly resolves at least two polymer size fractions.

CONCLUSIONS

Our results indicate that HDC has considerable potential for measurement of the molecular size and molecular size distribution of water-soluble polymers possessing high molecular weights. It is rather disappointing that long run times are necessary to avoid deformation and orientation of polymer molecules during separation. The lengthy experiment time makes operation of the apparatus difficult since detection of the polymer at low concentrations also

implies low signal levels. This signal can easily be lost in baseline drift for experiments that require tens of hours to complete.

Although other techniques may provide better molecular weight data and shorter analysis time, HDC still has considerable advantages in cost and simplicity. The major use of HDC in polymers will likely be for quality control. It has been to this purpose that the technique has found widest use as a tool for particle size analysis.

We would like to acknowledge financial support from the National Science Foundation Presidential Young Investigator Program (R. K. P.) and Graduate Fellowship Program (D. A. H.). Also, funds were provided by the Dow Chemical Co. A special thanks are due to Hamish Small of Dow (retired), who encouraged our efforts early on, and Mary Langhorst of Dow, who provided invaluable technical assistance. The data for TMV was provided by K. Larson and is included in her thesis.[32]

References

1. H. G. Barth, *J. Chromatogr. Sci.*, **18**, 409 (1980).
2. J. C. Giddings, G. Lin, and M. N. Myers, *J. Liq. Chromatogr.*, **1**, 1 (1978).
3. G. Holzwarth, *Carbohydr. Res.*, **66**, 173 (1978).
4. A. Keller and J. A. Odell, *Colloid Polym. Sci.*, **263**, 181 (1985).
5. T. Sato, T. Norisuye, and H. Fujita, *Polym. J.*, **16**, 341 (1984).
6. G. Halverson and M. Botty, *Am. Chem. Soc., Div. Polym. Mater. Sci.*, **51**, 548 (1984).
7. J. Klein and K. D. Conrad, *Makromol. Chem.*, **179**, 1635 (1978).
8. J. C. Giddings, *Adv. Chromatogr.*, **20**, 217 (1982).
9. G. Holzwarth, L. Soni, and D. N. Schulz, *Macromolecules*, **19**, 422 (1986).
10. H. Small, *J. Colloid Interface Sci.*, **48**, 147 (1974).
11. R. K. Prud'homme, G. Froiman, and D. A. Hoagland, *Carbohydr. Res.*, **106**, 225 (1982).
12. R. K. Prud'homme and D. A. Hoagland, *Separation Sci. Technol.*, **18**, 121 (1983).
13. J. Lecourtier and G. Chauvateau, *Macromolecules*, **17**, 1340 (1984).
14. R. Bird, W. E. Stewart, and E. N. Lightfoot, *Transport Phenomena*, Wiley, New York, 1960.
15. H. Brenner and L. J. Gaydos, *J. Colloid Interface Sci.*, **58**, 312 (1977).
16. D. J. Nagy, *J. Colloid Interface Sci.*, **93**, 590 (1983).
17. D. J. Shaw, *Introduction to Colloid and Surface Chemistry*, 3rd ed., Butterworths, Boston, 1980.
18. C. A. Silebi and A. J. McHugh, *Emulsions, Latices, and Dispersions*, P. Becher and M. N. Yudenfreund, Eds., Dekker, New York, 1978.
19. G. R. McGowan and M. A. Langhorst, *J. Colloid Interface Sci.*, **89**, 94 (1982).
20. N. Kawashima, N. Fujimoto, and K. Meguro, *J. Colloid Interface Sci.*, **103**, 459 (1985).
21. A. Homola and A. A. Robertson, *J. Colloid Interface Sci.*, **54**, 286 (1976).
22. M. A. Langhorst, F. W. Stanley, Jr., S. S. Cutie, J. H. Sugarman, L. R. Wilson, D. A. Hoagland, and R. K. Prud'homme, *Anal. Chem.*, **58**, 2242 (1986).
23. S. Saito and T. Taniguchi, *J. Colloid Interface Sci.*, **44**, 114 (1973).
24. J. -J. Lee and G. G. Fuller, *J. Colloid Interface Sci.*, **103**, 569 (1985).
25. J. S. King, W. Boyer, G. D. Wignall, and R. Ullman, in *Physical Optics of Dynamic Phenomena and Processes in Macromolecular Systems*, B. Sedlacek, Ed., de Gruyter, New York, 1985.
26. M. Muthukumar and S. F. Edwards, *J. Chem. Phys.*, **76**, 2720 (1982).
27. R. Haas and F. Durst, *Rheol. Acta*, **21**, 566 (1982).
28. W. W. Graessley, *Polymer*, **21**, 258 (1980).
29. C. F. Zukoski, Ph.D. thesis, Chemical Engineering Department, Princeton University, 1984.
30. M. Styring, C. Price, and C. Booth, *J. Chromatogr.*, **319**, 115 (1985).
31. M. Milas and M. Rinaudo, *Polym. Bull.*, **12**, 507 (1984).
32. K. A. Larson, Master's thesis, Chemical Engineering Department, Princeton University, 1983.
33. W. M. Kulicke and N. Bose, *Colloid Polym. Sci.*, **262**, 197 (1984).

34. H. G. Barth and F. J. Carlin, Jr., *J. Liq. Chromatogr.*, **7**, 1717 (1984).
35. F. Lambert, M. Milas, and M. Rinaudo, *Polym. Bull.*, **7**, 185 (1982).
36. S. Wellington, *Polym. Prepr. Am. Chem. Soc.*, **22**(2), 63 (1981).
37. T. Coviello, K. Kajiwara, W. Burchard, M. Dentini, and V. Crescenzi, *Macromolecules*, **19**, 2826 (1986).
38. W. -M. Kulicke and H. -H. Horl, *Colloid Polym. Sci.*, **263**, 530 (1985).
39. A. M. Basedow and K. H. Ebert, *Adv. Polym. Sci.*, **22**, 83 (1977).

Received May 1, 1987
Accepted November 2, 1987